Journal of Renewable Materials

Tech Science Press

DOI: 10.32604/jrm.2021.014584

ARTICLE

The Application of Cellulose Nanocrystals Modified with Succinic Anhydride under the Microwave Irradiation for Preparation of Polylactic Acid Nanocomposites

Ewa Szefer*, Agnieszka Leszczyńska, Edyta Hebda and Krzysztof Pielichowski

Department of Chemistry and Technology of Polymers, Cracow University of Technology, Krakow, 31-155, Poland

*Corresponding Author: Ewa Szefer. Email: ewa.szefer89@gmail.com

Received: 10 October 2020 Accepted: 18 January 2021

ABSTRACT

The aim of this work was to use cellulose nanocrystals that were obtained by hydrolysis in phosphoric acid solution and further modified with succinic anhydride in the microwave field for PLA reinforcement. A series of all-bionanocomposites containing unmodified and surface modified cellulose nanocrystals with CNC content in the range of 1–3 $\%_{w.t.}$ were obtained by melt blending and tested by XRD, SEM, DSC and DMA to investigate the effect of surface esterification of CNCs on the structure, morphology, dynamic mechanical properties of bionanocomposites, as well as phase transitions of PLA in the presence of cellulosic nanofiller. DMA investigations showed the highest increase of storage modulus by ca. 7% (335 MPa at 25°C) in the glassy state of PLA for 2 $\%_{w.t.}$ of unmodified CNC. Though, addition of 2 $\%_{w.t.}$ of succinylated CNCs caused the highest increase of the onset of glass transition temperature (by 6.2°C) thus widening the temperature range of biocomposite application. The increase of glass transition temperature indicates the strongest interfacial interactions due to improved miscibility of surface modified nanocrystals and thus good dispersion of additive in PLA matrix providing high interface.

KEYWORDS

Cellulose nanocrystals; CNC; whiskers; surface modification; succinic anhydride; PLA; polylactic acid; nanocomposites

1 Introduction

Nowadays, due to the growing concerns about the environment, there are extensive efforts dedicated to the use and development of 'green', eco-friendly additives such as cellulose nanomaterials (CNMs). CNMs are treated as a useful renewable and biodegradable replacement for usually used inorganic nanofillers such as clays or carbon nanotubes. Furthermore, they possess relevant advantages such as great specific strength and storage modulus in the range of 100–200 GPa [1]. Cellulose nanomaterials can be divided into two main groups, namely cellulose nanofibers (CNFs) and cellulose nanocrystals (CNCs) [2].

CNFs are nanosized in diameter and microsized in length flexible fibers. The ultimate characteristics and properties of the CNMs from different cellulose sources may differ; besides, synthesis conditions play an important role [2]. CNFs consist of 36 cellulose chains fibrils stacked in Iβ crystal structure, show a high aspect ratio as they have around 4–20 nm in width and around 500–2000 nm in length, and consist of both amorphous and crystalline phases [3]. The distinction between CNFs and microfibrillated cellulose depends on the fibrillation mechanism that leads to smaller diameters.

Cellulose nanocrystals have whisker shape and are usually isolated from native cellulose by precise hydrolysis process with mineral or organic acids. Hydrolysis of cellulose amorphous regions yields rod-like crystals with source-dependent diameters in the range of 5−50 nm, lengths around 100−3000 nm, and remarkably elastic modulus (∼105−168 GPa) [4−7]. The most common acid used for hydrolysis is sulphuric acid [8−12]. Since CNCs obtained by using sulphuric acid show moderate thermal stability, other acids have been applied. Product of cellulose hydrolysis with HCl display strong whisker-whisker interactions. For this reason, they quickly aggregate and it is are usually not easy to redisperse them in solvents or polymer matrices [13]. Amongst hydrolysing agents, phosphoric acid enables preparation of CNCs with improved thermal stability in comparison to sulphuric acid hydrolysis, and these CNCs show less aggregation tendency than CNCs obtained by hydrochloric acid hydrolysis [14−16].

The large interest in the nanocellulose as a reinforcing filler for composite materials originates from outstanding mechanical properties it demonstrates. Enhanced properties can often be reached for low filler volume fraction, without a detrimental effect on other properties such as impact resistance or plastic deformation capability [17]. Nevertheless, the main obstacle to the use of CNMs in polymer composite technology arises from the limited dispersibility of the polar filler in the hydrophobic composite matrix. In order to enhance the compatibility of a cellulose nanofiller, chemical modification is often needed [18]. Unmodified CNMs have a strong tendency to form larger structures via aggregation and agglomeration [19]. This is because nano scale particles with highly developed specific surface (S) have an increased thermodynamic potential (G), which is the cause of instability of nano objects.

Poor dispersion of the filler in the composite matrix deeply affects its mechanical properties. CNMs tends to form hydrogen bonds, which is why their dispersion is so difficult and challenging for composite applications. The redispersion of nanomaterials after drying is difficult, as irreversible aggregation of the nanoparticles occurs in a process known as “hornification,” which results in a material that cannot be used as a reinforcing nanofiller [20]. The main method for preventing hornification was the introduction of a steric barrier or electrostatic groups to block cooperative hydrogen bonding of the cellulose chains [21]. Versatility of hydroxyl groups at the surface of CNMs makes it simple to experiment with different chemical surface modifications using various techniques including esterification, etherification, oxidation, silylation and polymer grafting [22]. Such modifications show high efficiency in improving dispersibility of CNMs in polymer matrix and strengthening interfacial adhesion leading to better functional properties [23].

Among diverse chemical modifications, surface esterification represents one of the most promising technique. During the surface esterification, the reaction occurs at the outer side of CNMs leaving the cellulose crystalline structure in the interior intact. The surface modification reactions can be carried out exclusively under heterogeneous conditions [22]. The hydroxyl groups of cellulose can be esterified by reaction with acids or anhydrides, including succinic anhydride [14,15,18,24]. The reaction of cellulose with a cyclic anhydride, such as succinic anhydride, does not yield a by-product, leaving the modified polymer with covalently bonded carboxylic groups [14]. In the case of a reaction at temperatures above 100°C, the formation of diesters was observed, which resulted in cross-linking within the cellulose chains [25]. An interesting study of succinic anhydride surface modification was presented by Emam et al. where due to the esterification, the sorption was increased and the rate constant was raised from 10.82×10^{-3} min^{-1} to 20.27×10^{-3} min^{-1} for CNC and CNC-SA, respectively [24]. Succinylated cellulose nanocrystals, due to their excellent sorption capabilities, can be applied for removal of organic contaminations, e.g., methylene blue dye from water [26].

In general, microwave radiation is often used as an alternative input energy source, owing to its ability to rapidly generate heat. The esterification reaction of cellulose which receives energy by the conventional heating method takes longer periods of time for the reaction to be completed than microwave radiation

[18]. The effectiveness of microwaves as a heating source and its promoting effect on the esterification of cellulose has been widely examined [27−29].

The properties of poly(lactic acid) (PLA) depend on various factors, such as the origin, the production routes, and molar mass [1]. Moreover, thermal history influences on PLA crystalline degree and final properties. The PLA has some drawbacks such as relatively low thermal resistance, low glass transition, small crystallization rate and brittleness [30,31]. For this reason, adding nanofillers presents an appealing way to enhance the PLA properties. PLA reinforced with CNMs has received increased attention since both components are characterized by natural biodegradability and availability from renewable resources [32,33]. Among CNMs, cellulose nanocrystals are often used as a reinforcing additive thanks to its many assets described above. For example, Lee et al. obtained PLA/CNCs composites by functionalizing the bacterial cellulose (BC) to improve their homogenization [34]. Composite microspheres with 2 $\%_{w.t.}$ and 5 $\%_{w.t.}$ BC loading were fabricated, and the inclusion of organic acid functionalised BC into PLA induced an enhancement in tensile strength and modulus of the reinforced nanocomposites (by as much as 50% and 15% for 2 $\%_{w.t.}$ and 5 $\%_{w.t.}$ cellulose loading, respectively). Raquez et al. examined the consequences of cellulose surface modification by different chemical modifications, based on trialkoxysilanes to decorate CNCs with alkyl, amino and (meth)acryloxy moieties. Surface modified cellulose (3 $\%_{w.t.}$) was incorporated in the PLA matrix by direct melt-blending [35]. This research has shown that silane treatment manage to protect the CNCs additive structure intact by improving its thermo-stability and allows its extrusion. Among other substances used as compatibilizers, also anhydrides had been used before. For example, in the research conducted by Hong et al. maleic anhydride-grafted PLA was applied as compatibilizing factor to enhance the interfacial adhesion between polymer matrix and CNCs [36]. Preparation of PLA/CNC composites by melt-mixing were pursued by compression moulding process. The optimal processing settings were: 5 + 10 min, at 190° in order to prevent the PLA and CNCs degradation and also insufficient homogenization of the additive, which was checked by tensile experiments. The loading of cellulose additives (microcrystalline cellulose [MCC] and cellulose nanowhiskers [CNCs]) in PLA composites was 10 phr. Results showed that the tensile strength of the PLA/CNCs composite with 100 phr content of CNCs was 56.4% greater than the PLA/MCC composite also with 10 phr of MCC. Enhanced properties of CNCs/poly(butylene succinate) (PBS) composites were reported by Wu et al. [37]. In this study CNCs were obtained through sulfuric acid hydrolysis of MCC and then surface succinylation was performed in order to reduce nanomaterial's polarity. The results showed that better mechanical and thermal properties were found for composites with lower filler volume fractions. When modified CNCs were introduced at a loading lower than 3 $\%_{w.t.}$, the nanofiller was dispersed homogeneously in PBS matrix. Thereafter, when the filler content exceeded 3 $\%_{w.t.}$, both CNCs and succinylated CNCs showed more heavier self-aggregation and even phase separation.

Based on the literature reporting bio-nanocomposites obtained by melt mixing, an addition of 1–5 $\%_{w.t.}$ of nanocellulose in PLA composites results in substantial material's properties improvements. This is the reason why in this paper the focus is on composites with a lower filler weight content. The performance of succinylated CNCs as a reinforcing agent for PLA will be evaluated and compared with a series of PLA/unmodified CNCs bionanocomposites.

Summarizing, in this study CNCs were prepared through phosphoric acid hydrolysis of microcrystalline cellulose, and then surface modified with succinic anhydride (SA) in the microwave field and applied as a nanofiller in composites with a polylactide (PLA) matrix. A series of all-bionanocomposites containing unmodified and surface modified cellulose nanocrystals, at content in the range of 1–3 $\%_{w.t.}$ were obtained by melt blending and tested by XRD, SEM, DSC and DMA to investigate the effect of surface esterification of CNCs on the structure, morphology, dynamic mechanical properties of bionanocomposites, as well as phase transitions of PLA in the presence of cellulosic nanofiller.

2 Materials and Sample Preparation

2.1 Materials

Microcrystalline cellulose with a trade name Avicel PH-101 in a form of a white powder was acquired from Sigma Aldrich company (Darmstadt, Germany). This kind of cellulose has an average particle size 50 μm. Reagent grades of other chemicals such as phosphoric acid solution (85 $\%_{w.t.}$), pyridine, dimethylformamide, and succinic anhydride, were also produced by Sigma Aldrich company and used as received. For pre-reaction alkali treatment, analytical grade sodium hydroxide was used, purchased from Chempur, Poland.

Polylactic acid (PLA) granules in the form of pellets were provided by Nature Plast (PLI 003). According to the Material Safety Data Sheet, raw polymer has a melt flow index of value 12–20 g/10 min.

2.2 Preparation of Cellulose Materials

The preparation of nanocrystals was described in detail in our previous article [14]. Generally, microcrystalline cellulose was first purified twice by alkali treatment (2 h at 80°C with 5 $\%_{w.t.}$ sodium hydroxide solution). Afterwards, the residue was washed with distilled water to neutral pH. After purification step, 1 g of dried cellulose was mixed with distilled water. The mixture was cooled in an ice bath and phosphoric acid with a concentration of 76 $\%_{w.t.}$ was added via a dropping funnel. The hydrolysis reaction was carried out at temperature of 100°C for 90 min. The acid solution was removed from the cellulose nanocrystals (CNC_P series) by repeated centrifugation and then undergoing ultrasonic homogenisation with distilled water. Subsequently, the suspension was dialysed against distilled water for five days. Finally, the suspension was sonicated for 15 min and five drops of ethanol were added to reduce the crystallisation of water and agglomeration of CNCs during drying. Lastly, the dispersion was frozen using liquid nitrogen and freeze-dried in a FreeZone Plus 2.5 Labconoco freeze-dryer (Labconoco, Kansas City, MO, USA).

The cellulose nanocrystals obtained as described above were then modified with succinic anhydride (SA) under microwave irradiation condition at molar ratio of anhydride to hydroxyl groups of cellulose (SA:OH) of 5:1 and at temperature of 110°C. The succinylated CNCs were depicted as CNC_SA. Reaction was carried out in the Milestone RHS-2 multimodal microwave reactor. The 2 $\%_{w.t.}$ nanocellulose suspension was used for surface modification and prepared as follows: 0.5 g of dry CNCs and 16 ml of DMF were placed in a 100 ml three-necked flask with the stirrer in place. The flask was placed in a heating bowl with an integrated thermocouple and inert gas was connected. Initially, the mixture was preheated to 70°C. 10 ml of DMF was placed in a separate beaker and 7.42 g of succinic anhydride was dissolved therein. When the heated mixture reached the set temperature, the contents of the beaker were added to it, and then 0.026 ml of the pyridine as a catalyser was quickly added. Then the flask was immediately placed in a microwave reactor under nitrogen flow and magnetic mixing. Control temperature program consisted of two segments: 0.5 min dynamic segment with power 350 W and then 30 min isothermal segment with power 200 W at temperature of 110°C. The pyridine as a catalyst was added according to the study carried out by Sehaqui et al. [38]. After the modification, the reaction mixture was cooled down in an ice bath, residue was separated by centrifugation and then sonicated with distilled water. In order to purify the nanocellulose dispersion from the remaining reagents, it was again placed in a dialysis membrane for four days. In order to limit water crystallisation and aggregation of CNCs during freeze-drying process, tert-butanol was added to the water dispersion of nanocrystals to reach t-but:H_2O 1:5 (v/v) concentration [39]. Lastly, to obtain dry modified CNCs, the dispersion was also freeze-dried.

2.3 Preparation of PLA/CNC Nanocomposites

The pellets of PLA and cellulose aerogels of unmodified CNCs (CNC_P) and succinylated CNCs (CNC_SA) were dried in a laboratory vacuum drier at 60°C for 10 h. Then nanocomposites were

prepared using twin-screw ThermoScientific HAAKE Mini CTW extruder with a recycling channel allowing to control the residence time of the melt. The mini extruder has two temperature zones, and since it operated in the recycling mode, the temperatures in both zones were the same. Processing was carried out at melt temperature of 185°C and screw speed of 150 rpm. The content of cellulose nanocrystals were 1, 2 and 3 $\%_{w.t.}$. First the appropriate portion of PLA was melted and then the whiskers were immediately added to the polymer melt to avoid oxidative degradation of the filler. The dwell time during compounding of composites was 6 min. Then samples were further processed on an injection moulding machine ZAMAK WT 12 at barrel temperature of 185°C. The mould temperature was kept at 40°C. For the DSC, WAXD and DMA studies, injection-moulded sample bars were used.

3 Methods

3.1 Scanning Electron Microscopy (SEM)

Morphology of the cryo-fractured surface of the samples was examined using a JSM-6010LA Jeol Scanning Electron Microscope. The samples were metalized with gold-palladium using a Sputtering System Hummer 6.2 with the thickness of the layer being approximately 3 nm.

3.2 Fourier Transform Infrared (FTIR)

Fourier transform infrared spectra (FTIR) were recorded on the freeze-dried cellulose using the Thermo Scientific spectrophotometer model Nicolet iS5 with a C/ZnSe crystal, operating in an attenuated total reflectance mode (ATR). The measurement range for each sample was between 4000–450 cm^{-1} with scans number of 16 and resolution of 4 cm^{-1}.

3.3 X-Ray Diffraction (XRD)

X-ray diffraction measurements were performed using the Bruker D2 Phaser diffractometer at room temperature in the reflection mode (λ Cu Kα = 1.54 Å). Measurements were done in the range of 3°–40° with an increment of 0.02°. The crystallinity degree of cellulose samples was calculated as the ratio of the entire area of the crystalline peaks ($\sum_{Acrystal}$) to the sum of the areas of the crystalline peaks and the amorphous profile (($\sum_{Aamorphous}$) by the mathematical deconvolution done in the MagicPlot Student 2.7.1.freeware program according to Eq. (1):

$$x_c = \frac{\sum_{Acrystal}}{\sum_{Acrystal} + \sum_{Aamorphous}} \times 100 \tag{1}$$

The crystallinity degree of PLA in composites was determined by Bruker DIFFRAC.EVA software. The degree of crystallinity was calculated using the following Eqs. (2) and (3):

$$\%Amorphous = \frac{Global\ area - Reduced\ area}{Global\ area} \times 100$$

$$\%Crystallinity = 100 - \%Amorphous \tag{3}$$

where $\%Amorphous$ and $\%Crystallinity$ is the percentage of the amorphous and crystalline phases in the material, respectively; *Global area* is the total area under the WAXD curve and *Reduced area* is the area of the peak after background subtraction.

3.4 Differential Scanning Calorimetry (DSC)

Differential scanning calorimetry measurements were carried out using the Mettler Toledo DSC 822 apparatus in the temperature range from −75 to 190°C in an argon atmosphere with heating rate of 10 K/min. The glass transition temperature was determined by a midpoint on a step in the baseline of the measurement first and second heating curve. The degree of crystallinity (x_c) is calculated as follows [40]:

$$x_c = \frac{\Delta H_m - \Delta H_{cc}}{\Delta H_m^o \times (1 - x_D)} \times 100\% \quad (4)$$

where ΔH_m is measured change in melting enthalpy; x_D is the weight fraction of CNCs in the sample that does not undergo phase transformation in the polymer melting range; ΔH_{cc} is the cold crystallization enthalpy change and ΔH_m^o is the melting enthalpy of 100% crystalline PLA (value used 93 J/g [41]).

3.5 Dynamic Mechanical Analysis (DMA)

Dynamic mechanical analysis was carried out using DMA 242C Netzsch apparatus on the bars obtained by the injection moulding process (length 50 mm, width 10 mm, thickness 1 mm) in three-point bending mode (sample holder with 20 mm spacing between supports) under maximal dynamic force of 6 N, constant part of static force of 0.3 N, and static force 10% higher than dynamic. The maximal amplitude was set to 50 μm. A temperature scan from −30 to 140°C was performed at heating rate of 10 °C min^{-1} and with perturbation frequency of 1 Hz, under nitrogen atmosphere. Liquid nitrogen was used as cooling medium. The viscoelastic parameters of storage modulus (E′) were recorded as a function of temperature.

4 Results and Discussion

4.1 CNCs Filler Characteristics

The morphology of unmodified and surface modified CNCs was observed by SEM as shown in Figs. 1a and 1b, respectively. SEM microphotographs showed that the cellulose material obtained by hydrolysis in phosphoric acid solution displayed microporous aerogel morphology, while after their modification with succinic anhydride, better individualisation of the nanoparticles was observed. The presence of succinate groups on the surface of CNCs limited agglomeration upon drying probably by steric effects and repulsive interactions of negatively charged dissociated carboxylic groups [14]. FTIR spectrophotometry was used to monitor the reaction progress. The comparison of the absorbance FTIR spectra of the reference sample (CNC_P) and the post-reaction sample (CNC_SA) evidenced the presence of new ester groups. FTIR analysis of modified cellulose nanocrystal (Fig. 1c) confirmed partial esterification of hydroxyl groups on their surface by a presence of a new absorption band in modified samples at 1725 cm^{-1}. This band is related to carbonyl group stretching vibrations in esters bonds [42,43] and a broad peak at 1643 cm^{-1} can be assigned to the bending vibrations of adsorbed water [44,45]. XRD analysis of cellulose nanocrystals (Fig. 1d) showed that the reaction of CNCs with succinic anhydride leads to further hydrolysis of amorphous regions in cellulose nanomaterials. Modified sample exhibited higher content of crystalline fraction (79.4%) in comparison to hydrolyzed cellulose nanocrystals, for which this value was 74.9%. The increase in crystallinity can be advantageous from the point of view of using CNCs as reinforcement for PLA composites.

4.2 SEM Analysis of PLA/CNCs Composites

Since the mechanical properties of nanocomposites strongly depend on the interactions between the filler and the matrix that in turn depend on the dispersion degree of the filler [46], the scanning electron microscopy (SEM) was carried out in order to elucidate the dispersion state due to the interactions formed between CNCs and PLA. Fig. 2. shows the SEM images of the cryogenic fractured surfaces of neat PLA and PLA based bionanocomposites with 1 $\%_{w.t.}$ unmodified CNCs and modified CNCs at different loading. Neat PLA is characterized by smooth and uniform surface, similar to PLA with low loading of modified CNCs (2c) that showed surface typical of a semi-crystalline polymer with homogeneously dispersed filler. The good dispersion of modified nanocellulose could be due to the strong interaction between CNCs and PLA. A similar behaviour was also previously observed by Yang et al. [47]. Furthermore, the highest crystallinity degree of PLA_CNC_SA_1%, as reported below in discussion of DSC results, could be the indication for a better dispersion of filler in PLA [48]. Although, at lower

concentration (1 %w.t.) sample showed relatively small domains with a typical sea-island morphology, the increase in the CNCs concentration (3 %w.t.) caused formation of considerable amount of aggregates (2d). The fracture surface had more rough structure with higher number of micrometric aggregates suggesting that the interfacial adhesion between PLA and filler was not sufficient for breaking up aggregates at higher content of CNC_SA and the interparticulate interactions between whiskers were prevailing [49]. This could be the reason, why the mechanical properties of the sample PLA_CNC_SA_3% decreased, as discussed later in the mechanical properties section.

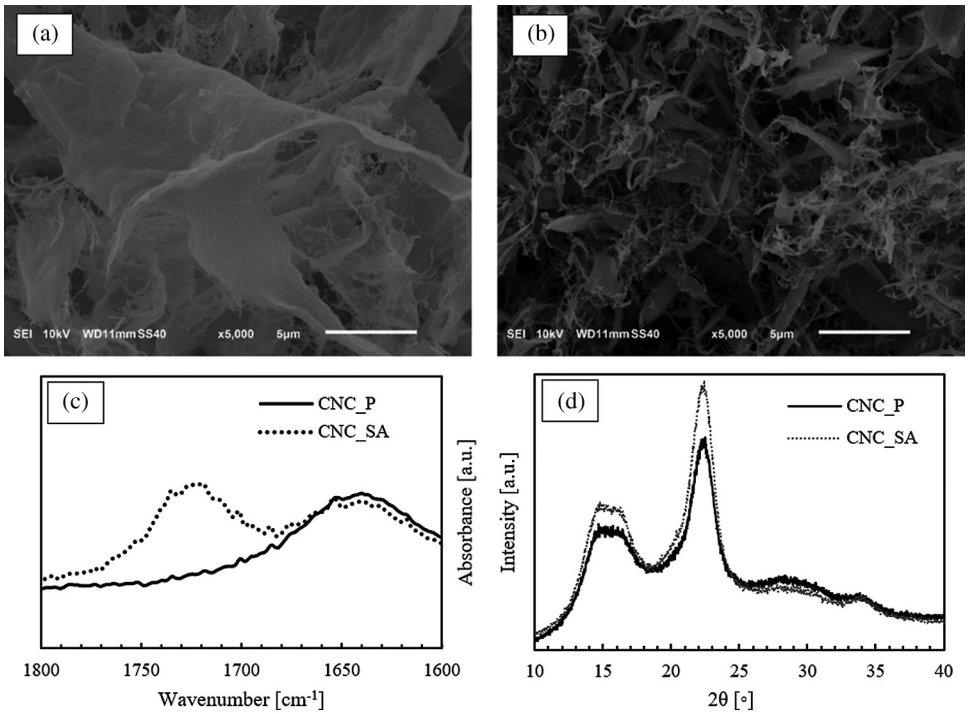

Figure 1: Morphological and structural characterization of cellulose nanofiller: 1a) and 1b) SEM microphotograph of aerogel of unmodified (CNC_P) and surface modified (CNC_SA) nanocrystalline cellulose, respectively; 1c) FTIR spectra of an unmodified CNCs (CNC_P) and after surface esterification with succinic anhydride (CNC_SA); 1d) WAXD patterns of unmodified (CNC_P) and modified (CNC_SA) nanocellulose

4.3 XRD Analysis of PLA/CNCs Composites

It is well-known that nanoparticles can influence the crystallization behaviour of semi-crystalline polymers. For example, dispersed nanosized montmorillonite particles act as a nucleating agent for PLA crystallization in the nanocomposite [50]. The physical and mechanical properties of a semi-crystalline polymer are controlled to some extent by polymer crystallinity and morphology [51]. Consequently, nanoparticles could impact the physical and mechanical properties. Nanoparticles can serve as heterogeneous nucleation sites for crystallization and act as effective nucleating agents [52]. The overall crystallization is governed by the competition between the nucleation effect and polymer chain mobility for crystalline growth [51].

The structures of pristine PLA and PLA biocomposites were characterized by X-ray diffraction (XRD) in order to study the effect of the nanocrystals type and content on the crystallinity of the PLA matrix. In Fig. 3a XRD patterns for PLA showed a wide band with a maximum at 2θ equal to 16.5°, giving the idea

of the dominating amorphous PLA nature [53]. Two peaks at 2θ around 16.5° and 22.4° were the most prominent in the biocomposites samples. These peaks are indicative of the PLA and cellulose crystallinities, respectively [54]. The peak at 22.4° subsides due to the low filler loading as well as being replaced by a broad shoulder next to it at around 16°, typical of a predominant amorphous material.

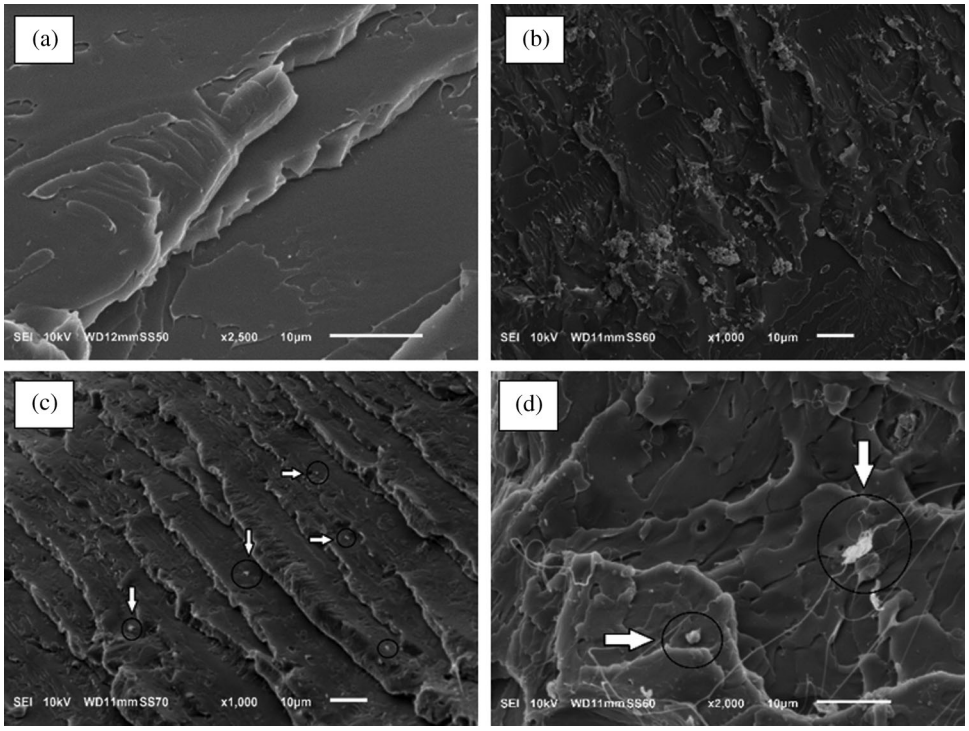

Figure 2: SEM images of the cryogenic fractured surfaces of neat PLA (2a); bionanocomposites with 1 $\%_{w.t.}$ of unmodified CNCs (2b); and different modified CNCs loading: PLA_CNC_SA_1% (2c); and PLA_CNC_SA_3% (2d), respectively

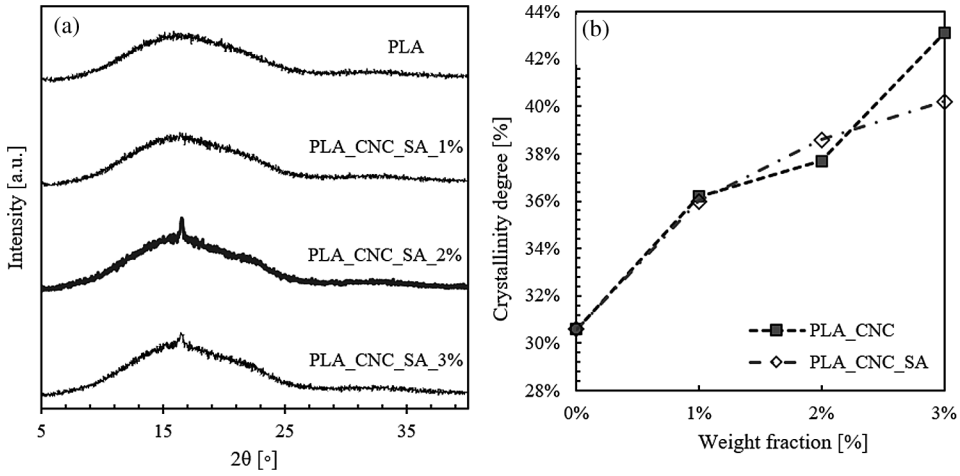

Figure 3: X-ray diffraction of pristine PLA and PLA/CNCs biocomposites at different content of modified cellulose nanocrystals (3a); and crystallinity degree from XRD measurements of PLA and PLA/CNC bionanocomposites (3b)

The crystallinity of PLA determined from the XRD diffraction patterns showed that CNCs could act as nucleating agent for PLA. Fig. 3b shows crystallinity degree trends for reference PLA and PLA composites with unmodified (PLA_CNC) and modified cellulose nanocrystals (PLA_CNC_SA).

4.4 DSC Studies of PLA/CNCs Composites

Differential scanning calorimetry was used to investigate the glass transition, crystallization and melting phenomena of PLA and PLA bionanocomposites and study the effect of CNC addition on the final properties of the obtained samples. DSC thermograms during first and second heating scans are shown in Fig. 4 while the thermal properties, such as glass transition temperature and the crystallinity degree calculated from first and second heating scans, are summarized in Tab. 1. The melting process of the PLA bionanocomposites containing unmodified and modified CNCs did not change significantly with respect to the pristine PLA matrix during the first heating scan. Only the sample with 2 $\%_{w.t.}$ of unmodified CNCs (PLA_CNC_2%) showed a slight a shift in the maximum peak of cold crystallization (T_{cc}) to higher temperature by about 4°C. The slight rise in T_m of composites could be caused by nucleating ability of CNCs to develop more heterogeneous crystalline morphology in PLA matrix. Similar conclusions were made in the research by Frone et al. [55] when cellulose nanofibers obtained by acid hydrolysis from commercially available MCC, were used as reinforcement in PLA matrix.

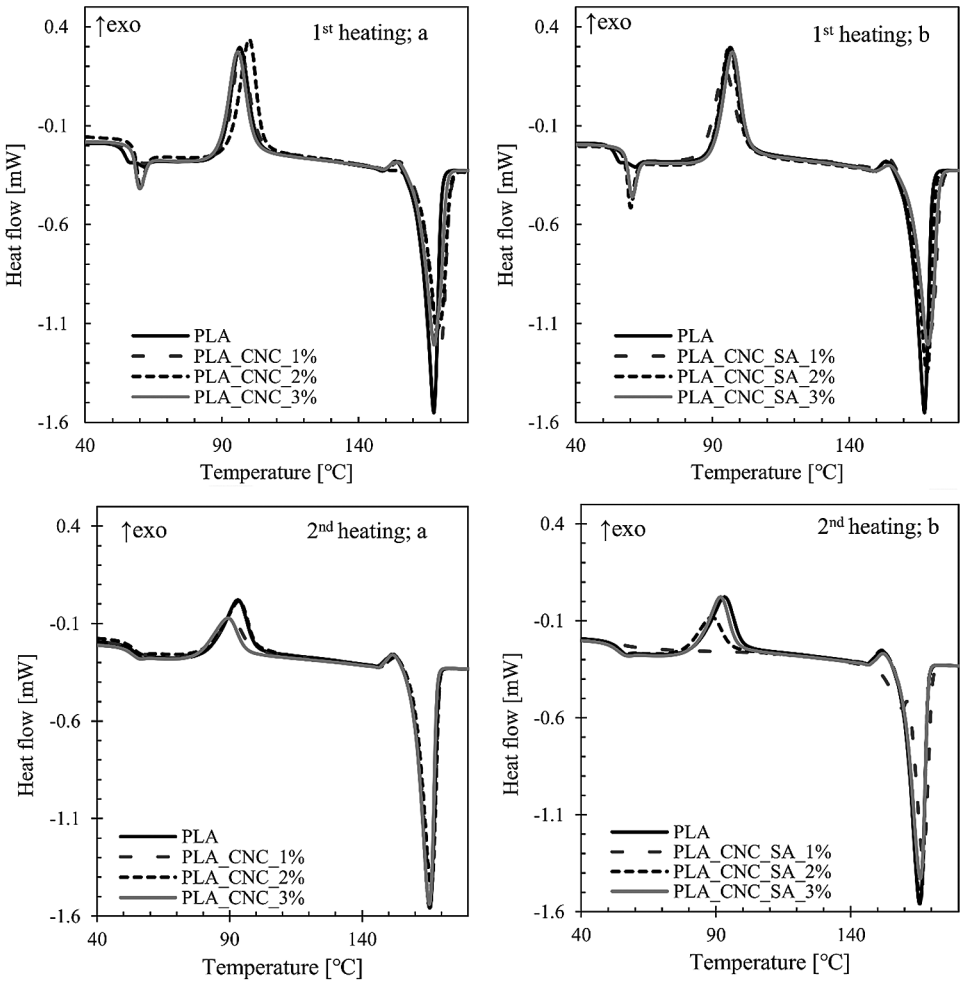

Figure 4: DSC scans for: 1st heating and 2nd heating for different filler weight contents of unmodified (a) and modified CNCs (b), respectively

Table 1: Thermal properties from DSC analysis of PLA and PLA bionanocomposites from the first and the second heating scan

Sample	T_g [°C]	ΔH_{cc} [J/g]	T_{cc} [°C]	ΔH_m [J/g]	T_m [°C]	x_c [%]
1st heating scan						
PLA	54.2	32.1	96.6	41.0	167.5	9.5
PLA_CNC_1%	57.4	31.9	97.1	39.5	169.5	8.2
PLA_CNC_2%	57.3	31.4	100.1	36.9	168.5	6.0
PLA_CNC_3%	57.0	31.3	95.7	37.0	167.5	6.3
PLA_CNC_SA_1%	56.9	30.0	94.5	40.1	168.9	10.9
PLA_CNC_SA_2%	57.3	31.2	96.1	37.7	168.3	7.1
PLA_CNC_SA_3%	57.5	29.9	97.2	37.3	168.9	8.2
2nd heating scan						
PLA	53.9	23.6	93.2	43.3	165.5	21.2
PLA_CNC_1%	53.6	14.2	91.2	42.1	165.7	30.3
PLA_CNC_2%	53.8	19.8	93.5	40.0	166.0	22.2
PLA_CNC_3%	52.0	15.8	89.3	41.5	165.3	28.5
PLA_CNC_SA_1%	53.7	–	–	43.0	166.7	46.7
PLA_CNC_SA_2%	52.9	14.2	88.5	40.9	165.6	29.3
PLA_CNC_SA_3%	52.9	20.8	91.8	38.9	165.7	20.1

During the second heating scan, the PLA bionanocomposites showed the higher values of crystallinity degree while the different ability to recrystallize after the cooling was highlighted by the low values of enthalpy or the absence of the registered cold crystallization. The main reasons for differences in the first and second heating scans can be the presence of residual moisture, as well as thermal history of the samples [56]. While all the obtained biocomposites showed higher degree of crystallinity during the second heating as compared to neat PLA, the sample with 1 $\%_{w.t.}$ of modified cellulose nanocrystals (PLA_CNC_SA_1%) had the highest degree of crystallinity for both the first and second heating. By analysing the trends one can be see that generally the higher the weight fraction of the nanofiller, the lower the degree of crystallinity.

The glass transition temperature (T_g) of PLA biocomposites is slightly higher than that of the neat PLA (Tab. 1).This indicates that the addition of CNCs leads to the reduction in PLA chain flexibility as T_g value is mainly related to the flexibility of polymeric segments [12]. Similar results were reported in works by Bulota et al. [57], and Baheti et al. [49], where TEMPO-oxidized cellulose and nanosized jute fiber were used as a reinforcement in PLA, respectively. Moreover, this phenomenon can be explained by hydrogen bonding interactions between hydroxyl groups from CNCs and carbonyl groups from PLA that cause a restricted polymer chain mobility. Consequently, the decrease in the polymer chain mobility associated with glass transition would increase the energy needed for this relaxation to occur [58].

The degree of crystallinity calculated from DSC and XRD showed different values. The discrepancy may result from fundamental difference in physical quantity measured by both methods. The change of enthalpy measured by DSC in the temperature range of PLA melting is a sum of heat effects of complex processes related to phase transitions upon heating—the endothermic heat of fusion and simultaneously running exothermic recrystallization of unperfect crystals and amorphous regions that may diminish the

total measured value of enthalpy change. XRD detects diffraction on the perfect crystal lattice but crystallinity evaluation by this method will miss the unperfect crystals, which, on the other hand, may produce heat effects detectable by DSC method. In our work the values of crystallinity calculated from XRD (Fig. 3b) were always higher than those calculated from DSC (Tab. 1). Similar effect was reported for PLA blends and it occurred due to the possible gradient in crystallinity degree in the surface and core of the injected bars [59]. XRD diffractograms just scanned the sample surface, while the DSC evaluated the bulk crystallinity [60]. In consequence the crystallinity degree values from XRD measurements were strongly influenced by injection moulding. During injection moulding the polymer melt was subjected to higher shearing and cooling rates in the skin layer of sample bars as compared to the core material [61]. Forced alignment of macromolecules in the skin layer along the direction of melt flow influence the morphology and favours growth of crystals due to molecules orientation leading to higher crystallinity [60].

4.5 Thermo-Mechanical Properties of PLA/CNCs Composites

Dynamic mechanical analysis (DMA) can explain the reinforcing effect of the modified CNCs by measuring the storage modulus as a function of temperature. The influence of cellulose nanomaterial concentration in PLA matrix on the storage modulus (E′) was shown in the Fig. 5. Results obtained from DMA analysis showed that the reference sample had lower values of storage modulus as compared to all of the PLA composites except the sample with the highest concentration of unmodified cellulose nanocrystals (PLA_CNC_3%). This drop in storage modulus is attributed to the aggregation and agglomeration of CNCs in PLA. These aggregates could act as stress-centralized point and reduced the surface area interaction between CNCs and PLA which consequently leads to decrease in the mechanical properties of this nanocomposite [12].

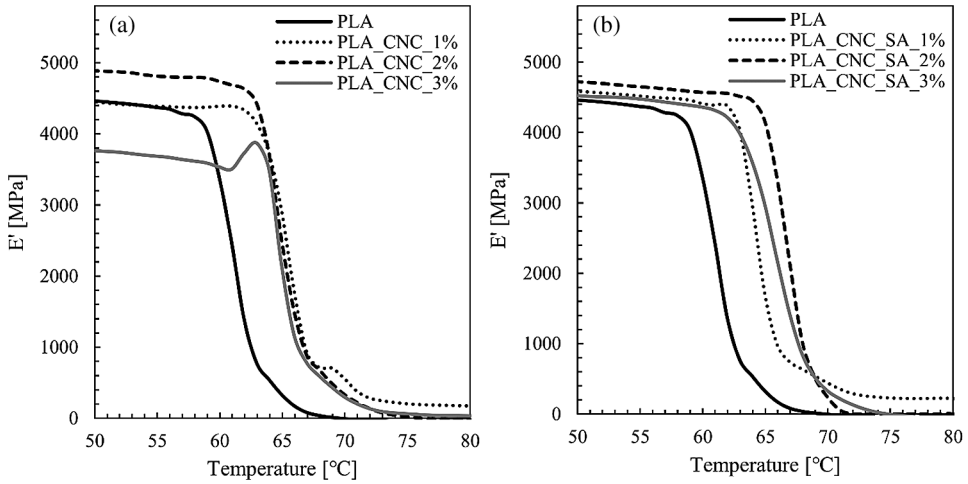

Figure 5: Storage modulus vs temperature for PLA and its composites with unmodified (a); and modified (b) CNCs at 1 Hz frequency in the temperature region of glass transition

Tab. 2 shows the detailed values of storage modulus at approximately room temperature (25°C) and glass transition temperature (T_g) determined from storage modulus onset of PLA and PLA bionanocomposites. The glass transition temperature determined by the DSC method is slightly lower than that of the DMA method, which may be influenced by the different measuring mechanisms [62]. DSC registers the change in thermal enthalpy, while DMA method measures the shift of mechanical modulus. Although it is generally agreed that both methods could be used to characterize the glass transition temperature of polymeric materials, the Tg data collected from the DSC and DMA could not be

compared directly [62]. The onset of PLA glass transition is indicative of the temperature range of practical material use in structural applications within which the material demonstrates relatively constant mechanical performance. The glass transition relaxation is associated with a drastic drop in PLA stiffness occurring in narrow temperature range of ca. 5°C. According to DMA analysis, all the nanocomposite samples displayed a significant increase in the glass transition temperature when compared to the neat PLA, which was assigned to a reduction in polymer chain mobility. It is believed that CNCs act as physical interlocking points in the matrix that limit chain mobility [63]. For instance, the highest glass transition temperature was determined for sample with 2%$_{w.t.}$ loading of modified CNCs (PLA_CNC_SA_2%), while the best mechanical properties were found for sample with the same filler loading, but with unmodified nanocrystals (PLA_CNC_2%). For this sample, an improvement in the storage modulus at room temperature was noted of about 350 MPa. This enhancement has been attributed to the good dispersion, stiffness of the filler, and developed interface. Consequently, filler-matrix interactions became more pronounced and better interfacial adhesion was formed between the filler and the matrix. For this reason, the stress transfers to the nanofiller, which is the load bearing matter, becomes efficient and then improve the mechanical strength [49].

Table 2: Storage modulus at 25°C and glass transition temperature (T_g) determined from storage modulus onset of PLA and PLA bionanocomposites

Sample	Tg [°C]	E′ [MPa] at 25°C
PLA	58.4	4788
PLA_CNC_1%	63.0	4714
PLA_CNC_2%	62.7	5123
PLA_CNC_3%	63.8	4066
PLA_CNC_SA_1%	62.6	4864
PLA_CNC_SA_2%	64.6	5026
PLA_CNC_SA_3%	62.9	4748

5 Conclusions

PLA nano-biocomposites reinforced with unmodified and modified cellulose nanocrystals were successfully prepared by extrusion method and the effect of the CNCs amount in the composite and surface functionalization by esterification with succinic anhydride on the structural and thermal properties of nanocomposites was investigated.

SEM analysis showed the good dispersion of modified CNCs at low concentrations indicating that the surface esterification allowed the better dispersion of the CNC in the PLA matrix.

The crystallinity of PLA determined from the XRD diffraction patterns showed that CNCs could act as nucleating agent for PLA.

The melting process of the PLA bionanocomposites containing unmodified and modified CNCs did not change significantly with respect to the pristine PLA matrix during the DSC first heating scan. While all the obtained biocomposites showed higher degree of crystallinity during the second heating as compared to neat PLA, the sample with 1 %$_{w.t.}$ of modified cellulose nanocrystals (PLA_CNC_SA_1%) had the highest degree of crystallinity for both the first and second heating. By analysing the trends one can be see that generally the higher the weight fraction of the nanofiller, the lower the degree of crystallinity. The glass transition temperature (Tg) of PLA biocomposites is slightly higher than that of the neat PLA. This indicates that

the addition of CNCs leads to the reduction in PLA chain flexibility as Tg value is mainly related to the flexibility of polymeric segments.

DMA investigations performed on PLA/modified CNCs samples showed that adding 2 $\%_{w.t.}$ of modified cellulose nanocrystals into PLA causes an increase of storage modulus values. Moreover, all of the nanocomposite samples displayed a significant increase in the glass transition temperature when compared to the neat PLA sample. The highest increase of glass transition temperature was observed for sample containing 2 $\%_{w.t.}$ of succinylated CNC. This indicates the strongest interfacial interactions due to improved miscibility of surface modified nanocrystals and thus obtained good dispersion of additive in PLA matrix providing high interface.

Funding Statement: The authors received no specific funding for this study.

Conflicts of Interest: The authors declare that they have no conflicts of interest to report regarding the present study.

References

1. Mokhena, T. C., Sefadi, J. S., Sadiku, E. R., John, M. J., Mochane, M. J. et al. (2018). Thermoplastic processing of PLA/cellulose nanomaterials composites. *Polymers, 10(12),* 1363. DOI 10.3390/polym10121363.
2. Kargarzadeh, H., Mariano, M., Gopakumar, D., Ahmad, I., Thomas, S. et al. (2018). Advances in cellulose nanomaterials. *Cellulose, 25(4),* 2151–2189. DOI 10.1007/s10570-018-1723-5.
3. Moon, R. J., Martini, A., Nairn, J., Simonsen, J., Youngblood, J. (2011). Cellulose nanomaterials review: Structure, properties and nanocomposites. *Chemical Society Reviews, 40(7),* 3941. DOI 10.1039/c0cs00108b.
4. Araki, J., Wada, M., Kuga, S. (2001). Steric stabilization of a cellulose microcrystal suspension by poly(ethylene glycol) grafting. *Langmuir, 17(1),* 21–27. DOI 10.1021/la001070m.
5. Sturcová, A., Davies, G. R., Eichhorn, S. J. (2005). Elastic modulus and stress-transfer properties of tunicate cellulose whiskers. *Biomacromolecules, 6(2),* 1055–1061. DOI 10.1021/bm049291k.
6. De Souza Lima, M. M., Wong, J. T., Paillet, M., Borsali, R., Pecora, R. (2003). Translational and rotational dynamics of rodlike cellulose whiskers. *Langmuir, 19(1),* 24–29. DOI 10.1021/la020475z.
7. Rusli, R., Eichhorn, S. J. (2008). Determination of the stiffness of cellulose nanowhiskers and the fiber-matrix interface in a nanocomposite using Raman spectroscopy. *Applied Physics Letters, 93(3),* 033111. DOI 10.1063/1.2963491.
8. Lahiji, R. R., Xu, X., Reifenberger, R., Raman, A., Rudie, A. et al. (2010). Atomic force microscopy characterization of cellulose nanocrystals. *Langmuir, 26(6),* 4480–4488. DOI 10.1021/la903111j.
9. Siaueira, G., Bras, J., Dufresne, A. (2009). Cellulose whiskers versus microfibrils: Influence of the nature of the nanoparticle and its surface functionalization on the thermal and mechanical properties of nanocomposites. *Biomacromolecules, 10(2),* 425–432. DOI 10.1021/bm801193d.
10. Fan, J. S., Li, Y. H. (2012). Maximizing the yield of nanocrystalline cellulose from cotton pulp fiber. *Carbohydrate Polymers, 88(4),* 1184–1188. DOI 10.1016/j.carbpol.2012.01.081.
11. Tang, Y., Yang, S., Zhang, N., Zhang, J. (2014). Preparation and characterization of nanocrystalline cellulose via low-intensity ultrasonic-assisted sulfuric acid hydrolysis. *Cellulose, 21(1),* 335–346. DOI 10.1007/s10570-013-0158-2.
12. Haafiz, M. K. M., Hassan, A., Khalil, H. A., Fazita, M. R. N., Islam, S. et al. (2016). Exploring the effect of cellulose nanowhiskers isolated from oil palm biomass on polylactic acid properties. *International Journal of Biological Macromolecules, 85(2),* 370–378. DOI 10.1016/j.ijbiomac.2016.01.004.
13. Van den Berg, O., Capadona, J. R., Weder, C. (2007). Preparation of homogeneous dispersions of tunicate cellulose whiskers in organic solvents. *Biomacromolecules, 8(4),* 1353–1357. DOI 10.1021/bm061104q.
14. Leszczyńska, A., Radzik, P., Szefer, E., Mičušík, M., Omastová, M. et al. (2019). Surface modification of cellulose nanocrystals with succinic anhydride. *Polymers, 11(5),* 866. DOI 10.3390/polym11050866.

15. Leszczyńska, A., Radzik, P., Haraźna, K., Pielichowski, K. (2018). Thermal stability of cellulose nanocrystals prepared by succinic anhydride assisted hydrolysis. *Thermochimica Acta, 663,* 145–156. DOI 10.1016/j.tca.2018.03.015.
16. Trache, D., Haaflt, M., Hussin, M. H., Thakur, V. K. (2017). Recent progress in cellulose nanocrystals: Sources and production. *Nanoscale, 9(5),* 1763–1786. DOI 10.1039/C6NR09494E.
17. Dufresne, A. (2008). Cellulose-based composites and nanocomposites. In: Belgacem, M. N., Gandini, A. (eds.), *Monomers, Polymers and Composites from Renewable Resources,* pp. 401–418. Philadelphia, PA: Elsevier Science.
18. Szefer, E., Leszczyńska, A., Pielichowski, K. (2018). Modification of microcrystalline cellulose filler with succinic anhydride—effect of microwave and conventional heating. *Composites Theory and Practice, 18(1),* 25–31.
19. Ioelovich, M. (2008). Nanostructured cellulose: Review. *BioResources, 3,* 1403–1418.
20. Islam, M. T., Alam, M. M., Zoccola, M. (2013). Review on modification of nanocellulose for application in composites. *International Journal of Innovative Research in Science, Engineering and Technology, 2,* 10.
21. Klemm, D., Heublein, B., Fink, H. P., Bohn, A. (2005). Cellulose: Fascinating biopolymer and sustainable raw material. *Angewandte Chemie International Edition, 44(22),* 3358–3393. DOI 10.1002/anie.200460587.
22. Wang, Y., Wang, X., Xie, Y., Zhang, K. (2018). Functional nanomaterials through esterification of cellulose: A review of chemistry and application. *Cellulose, 25(7),* 3703–3731. DOI 10.1007/s10570-018-1830-3.
23. Fujisawa, S., Saito, T., Kimura, S., Iwata, T., Isogai, A. (2013). Surface engineering of ultrafine cellulose nanofibrils toward polymer nanocomposite materials. *Biomacromolecules, 14(5),* 1541–1546. DOI 10.1021/bm400178m.
24. Emam, H. E., Shaheen, T. I. (2019). Investigation into the role of surface modification of cellulose nanocrystals with succinic anhydride in dye removal. *Journal of Polymers and the Environment, 27(11),* 2419–2427. DOI 10.1007/s10924-019-01533-9.
25. Hill, C. (2006). *Wood modification: Chemical, thermal and other processes,* pp. 79–83. Wiley.
26. George, A. L., White, G. F. (1999). Optimization of the methylene blue assay for anionic surfactants added to estuarine and marine water. *Environmental Toxicology and Chemistry, 18(10),* 2232–2236. DOI 10.1002/etc.5620181016.
27. Casarano, R., El Seoud, O. A. (2013). Successful application of an ionic liquid carrying the fluoride counter-ion in biomacromolecular chemistry: Microwave-assisted acylation of cellulose in the presence of 1-allyl-3-methylimidazolium fluoride/DMSO mixtures. *Macromolecular Bioscience, 13(2),* 191–202. DOI 10.1002/mabi.201200296.
28. Mai, X. T., Appiah-Ntiamoah, R., Momade, F. W. Y., Kim, H. (2012). Esterification of cellulose with palmitoyl chloride by using microwave irradiation and application to adsorption of methylene blue. *Advanced Materials Research, 622–623,* 1768–1773. DOI 10.4028/www.scientific.net/AMR.622-623.1768.
29. Jandura, P., Kokta, B. V., Riedl, B. (2000). Fibrous long-chain organic acid cellulose esters and their characterization by diffuse reflectance FTIR spectroscopy, solid-state CP/MAS carbon-13 NMR, and x-ray diffraction. *Journal of Applied Polymer Science, 78,* 1354–1365.
30. Scaffaro, R., Botta, L., Lopresti, F., Maio, A., Sutera, F. (2017). Polysaccharide nanocrystals as fillers for PLA based nanocomposites. *Cellulose, 24(2),* 447–478. DOI 10.1007/s10570-016-1143-3.
31. Fortunati, E., Puglia, D., Iannoni, A., Terenzi, A., Kenny, J. M. et al. (2017). Processing conditions, thermal and mechanical responses of stretchable poly (lactic acid)/poly (butylene succinate) films. *Materials, 10(7),* 809. DOI 10.3390/ma10070809.
32. Oksman, K., Aitomaki, Y., Mathew, A. P., Siqueira, G., Zhou, Q. et al. (2016). Review of the recent developments in cellulose nanocomposite processing. *Composites Part A: Applied Science and Manufacturing, 83(5),* 2–18. DOI 10.1016/j.compositesa.2015.10.041.
33. Armentano, I., Bitinis, N., Fortunati, E., Mattioli, S., Rescignano, N. et al. (2013). Multifunctional nanostructured PLA materials for packaging and tissue engineering. *Progress in Polymer Science, 38(10–11),* 1720–1747. DOI 10.1016/j.progpolymsci.2013.05.010.

34. Lee, K. Y., Blaker, J. J., Bismarck, A. (2009). Surface functionalisation of bacterial cellulose as the route to produce green polylactide nanocomposites with improved properties. *Composites Science and Technology, 69 (15–16),* 2724–2733. DOI 10.1016/j.compscitech.2009.08.016.
35. Raquez, J. M., Murena, Y., Goffin, A. L., Habibi, Y., Ruelle, B. et al. (2012). Surface-modification of cellulose nanowhiskers and their use as nanoreinforcers into polylactide: A sustainably-integrated approach. *Composites Science and Technology, 72(5),* 544–549. DOI 10.1016/j.compscitech.2011.11.017.
36. Hong, J., Kim, D. S. (2013). Preparation and physical properties of polylactide/cellulose nanowhisker/nanoclay composites. *Polymer Composites, 34(2),* 293–298. DOI 10.1002/pc.22413.
37. Wu, C., Zhang, X., Wang, X., Gao, Q., Li, X. (2019). Surface modification of cellulose nanocrystal using succinic anhydride and its effects on poly(butylene succinate) based composites. *Cellulose, 26(5),* 3167–3181. DOI 10.1007/s10570-019-02292-5.
38. Sehaqui, H., Kulasinski, K., Pfenninger, N., Zimmermann, T., Tingaut, P. (2016). Highly carboxylated cellulose nanofibers via succinic anhydride esterification of wheat fibers and facile mechanical disintegration. *Biomacromolecules, 18(1),* 242–248. DOI 10.1021/acs.biomac.6b01548.
39. Liu, C., Li, B., Du, H., Lv, D., Zhang, Y. et al. (2016). Properties of nanocellulose isolated from corncob residue using sulfuric acid, formic acid, oxidative and mechanical methods. *Carbohydrate Polymers, 151(6),* 716–724. DOI 10.1016/j.carbpol.2016.06.025.
40. Lizundia, E., Fortunati, E., Dominici, F., Vilas, J. L., León, L. M. et al. (2016). PLLA-grafted cellulose nanocrystals: Role of the CNC content and grafting on the PLA bionanocomposite film properties. *Carbohydrate Polymers, 142(10–11),* 105–113. DOI 10.1016/j.carbpol.2016.01.041.
41. Cao, X., Mohamed, A., Gordon, S. H., Willett, J. L., Sessa, D. J. (2003). DSC study of biodegradable poly(lactic acid) and poly(hydroxy ester ether) blends. *Thermochimica Acta, 406(1–2),* 115–127. DOI 10.1016/S0040-6031 (03)00252-1.
42. Moronkola, B. A., Moronkola, D. O., Iwoye, A. (2011). Studies on the isolation, structural and functional properties of Starch Succinate of Cocoyam (Colocasia antiquorum). *Der Chemica Sinica, 2,* 228–244.
43. Mannan, T. M., Soares, J. B. P., Berry, R. M., Hamad, W. Y. (2016). *In-situ* production of polyethylene/cellulose nanocrystal composites. *Canadian Journal of Chemical Engineering, 94(11),* 2107–2113. DOI 10.1002/cjce.22608.
44. Fengel, D. (1993). Influence of water on the OH valency range in deconvoluted FTIR spectra of cellulose. *Holzforschung, 47(2),* 103–108. DOI 10.1515/hfsg.1993.47.2.103.
45. Gierlinger, N., Schwanninger, M., Reinecke, A., Burgert, I. (2006). Molecular changes during tensile deformation of single wood fibers followed by Raman microscopy. *Biomacromolecules, 7(7),* 2077–2081. DOI 10.1021/bm060236g.
46. Kemala, T., Budianto, E., Soegiyono, B. (2012). Preparation and characterization of microspheres based on blend of poly(lactic acid) and poly(ε-caprolactone)with poly(vinyl alcohol) as emulsifier. *Arabian Journal of Chemistry, 5(1),* 103–108. DOI 10.1016/j.arabjc.2010.08.003.
47. Yang, W., Dominici, F., Fortunati, E., Kenny, J. M., Puglia, D. (2015). Melt free radical grafting of glycidyl methacrylate (GMA) onto fully biodegradable poly(lactic) acid films: Effect of cellulose nanocrystals and a masterbatch process. *RSC Advances, 5(41),* 32350–32357. DOI 10.1039/C5RA00894H.
48. Haafiz, M. K. M., Hassan, A., Zakaria, Z., Inuwa, I. M. (2014). Isolation and characterization of cellulose nanowhiskers from oil palm biomass microcrystalline cellulose. *Carbohydrate Polymers, 103(2),* 119–125. DOI 10.1016/j.carbpol.2013.11.055.
49. Baheti, V., Militky, J., Marsalkova, M. (2013). Mechanical properties of poly lactic acid composite films reinforced with wet milled jute nanofibers. *Polymer Composites, 34(12),* 2133–2141. DOI 10.1002/pc.22622.
50. Nam, J. Y., Ray, S. S., Okamoto, M. (2003). Crystallization behavior and morphology of biodegradable polylactide/layered silicate nanocomposite. *Macromolecules, 36(19),* 7126–7131. DOI 10.1021/ma034623j.
51. Kamal, M. R., Khoshkava, V. (2015). Effect of cellulose nanocrystals (CNC) on rheological and mechanical properties and crystallization behavior of PLA/CNC nanocomposites. *Carbohydrate Polymers, 123(15),* 105–114. DOI 10.1016/j.carbpol.2015.01.012.
52. Ghasemi, H., Carreau, P. J., Kamal, M. R. (2012). Isothermal and non-isothermal crystallization behavior of PET nanocomposites. *Polymer Engineering & Science, 52(2),* 372–384. DOI 10.1002/pen.22092.

53. Fortunati, E., Peltzer, M., Armentano, I., Torre, L., Jiménez, A. et al. (2012). Effects of modified cellulose nanocrystals on the barrier and migration properties of PLA nano-biocomposites. *Carbohydrate Polymers, 90(2),* 948–956. DOI 10.1016/j.carbpol.2012.06.025.

54. Hossain, K. M. Z., Ahmed, I., Parsons, A. J., Scotchford, C. A., Walker, G. S. et al. (2012). Physico-chemical and mechanical properties of nanocomposites prepared using cellulose nanowhiskers and poly(lactic acid). *Journal of Materials Science, 47(6),* 2675–2686. DOI 10.1007/s10853-011-6093-4.

55. Frone, A. N., Berlioz, S., Chailan, J. F., Panaitescu, D. M. (2013). Morphology and thermal properties of PLA–cellulose nanofibers composites. *Carbohydrate Polymers, 91(1),* 377–384. DOI 10.1016/j.carbpol.2012.08.054.

56. Hossain, K. M. Z., Jasmani, L., Ahmed, I., Parsons, A. J., Scotchford, C. A. et al. (2012). High cellulose nanowhisker content composites through cellosize bonding. *Soft Matter, 8(48),* 12099–12110. DOI 10.1039/c2sm26912k.

57. Bulota, M., Vesterinen, A. H., Hughes, M., Seppala, J. (2013). Mechanical behavior, structure, and reinforcement processes of TEMPO-oxidized cellulose reinforced poly(lactic) acid. *Polymer Composites, 34(2),* 173–179. DOI 10.1002/pc.22390.

58. Liu, M., Zhang, Y., Zhou, C. (2013). Nanocomposites of halloysite and polylactide, Meshless Local Patrov-Galerkin (MLPG) approaches for weaklysingular traction & displacement boundary integral equations. *Applied Clay Science, 75–76(5),* 52–59. DOI 10.1016/j.clay.2013.02.019.

59. Carrasco, F., Pagès, P., Gámez-Pérez, J., Santana, O. O., Maspoch, M. L. (2010). Processing of poly(lactic acid): Characterization of chemical structure, thermal stability and mechanical properties. *Polymer Degradation and Stability, 95(2),* 116–125. DOI 10.1016/j.polymdegradstab.2009.11.045.

60. Kaavessina, M., Ali, I., Al-Zahrani, S. M. (2012). The influences of elastomer toward crystallization of poly(lactic acid). *Procedia Chemistry, 4,* 164–171. DOI 10.1016/j.proche.2012.06.023.

61. Pielichowski, K., Leszczyńska, A. (2006). Polyoxymethylene-based nanocomposites with montmorillonite: An introductory study. *Polimery, 51(2),* 143–149. DOI 10.14314/polimery.2006.143.

62. Zhang, J. L., Zhang, X. Q., Li, M. C., Dong, J., Lee, S. Y. et al. (2019). Cellulose nanocrystal driven microphase separated nanocomposites: Enhanced mechanical performance and nanostructured morphology. *International Journal of Biological Macromolecules, 130,* 685–694. DOI 10.1016/j.ijbiomac.2019.02.159.

63. Zhang, J. L., Li, M. C., Zhang, X. Q., Ren, S. X., Dong, L. L. et al. (2019). Surface modified cellulose nanocrystals for tailoring interfacial miscibility and microphase separation of polymer nanocomposites. *Cellulose, 26(7),* 4301–4312. DOI 10.1007/s10570-019-02379-z.